Tucker Tensor Decomposition of Multi-session EEG Data

Zuzana Rošťáková(✉), Roman Rosipal, and Saman Seifpour

Institute of Measurement Science, Slovak Academy of Sciences,
Dúbravská cesta 9, 841 04 Bratislava, Slovakia
zuzana.rostakova@savba.sk

Abstract. The Tucker model is a tensor decomposition method for multi-way data analysis. However, its application in the area of multi-channel electroencephalogram (EEG) is rare and often without detailed electrophysiological interpretation of the obtained results. In this work, we apply the Tucker model to a set of multi-channel EEG data recorded over several separate sessions of motor imagery training. We consider a three-way and four-way version of the model and investigate its effect when applied to multi-session data. We discuss the advantages and disadvantages of both Tucker model approaches.

Keywords: Multi-channel electroencephalogram · Sensorimotor rhythms · Tucker model

1 Introduction

A compact and physiologically interpretable representation and analysis of electroencephalographic (EEG) data represent a challenging task. An important part of EEG analysis is the detection of latent sources of rhythmic activity in the time-varying EEG spectrum. For this purpose, the frequency decomposition of EEG signals, like the fast Fourier (FFT) or wavelet transform (WT), is often used. The time modality is often represented by a sequence of short EEG windows at which the frequency decomposition is applied. Finally, because EEG is often recorded at multiple electrodes, the third important modality is space, represented by different montages of EEG electrodes on the scalp. Other modalities often associated with EEG data analysis are the separation of subjects into different groups (male vs female, healthy vs patient, etc.) or experiments with a set of, in time separated, recorded sessions (different days, blocks of trials, etc.), to name a few. Therefore, the arrangement of EEG data into a multi-way array (a tensor) and application of the proper multi-way array decomposition method represents a natural way to analyse EEG data [3,7].

This contrasts with a set of traditional methods, for example, the principal component analysis (PCA) or independent component analysis (ICA), which operates on a two-way array where different modalities are concatenated into a single-mode (frequency and space or time and space, etc.).

I. Farkaš et al. (Eds.): ICANN 2020, LNCS 12396, pp. 115–126, 2020.
https://doi.org/10.1007/978-3-030-61609-0_10

The most frequently used tensor decomposition methods are the parallel factor analysis (PARAFAC) [5] and the Tucker model [12]. In both models, a multi-way array is decomposed into a set of interpretable matrices representing latent sources of variability present in data.

In the study, we focus on the tensor decomposition of EEG data with the aim of detection, monitoring, and analysis of latent sensorimotor EEG rhythms activated during motor imagery-based neurofeedback training of patients with hemiplegia due to a stroke.

We already successfully demonstrated the usefulness of PARAFAC when applied to multi-channel EEG data [9,10]. However, in these studies, each subject and each training session data were analysed separately, and the subject-specific PARAFAC latent factors, common across all training sessions, were detected in a semi-automatic way by using a combined data clustering and visual inspection approach. Therefore, it is reasonable to ask if these common latent factors, referred to as 'atoms', could be extracted by analysing the combined data pooled across all training sessions and in one step. Note, in our experimental design, a session represents motor imagery-based training on a separate day.

Following the previous detailed analysis of identified EEG rhythms across days and subjects [9], we hypothesise, that simultaneous analysis of all training sessions may lead to the direct detection of subject-specific atoms, which would closely match the ones extracted using a single session approach. To do this, it turns to be natural to rearrange EEG data into a four-way tensor representing time, space, frequency, and session modes. However, the training sessions do not share common patterns in the time domain, because the number of motor imagery tasks and the subject's performance varies across days. In other words, the value representing a session needs to be considered as a qualitative, not quantitative, variable in the four-way tensor arrangement. This also leads to the second form of data representation where data across the time mode are concatenated and create one large three-way tensor.[1]

In this study, we discuss the advantages and disadvantages of the two approaches and validate their performance to detect subject-specific motor imagery related EEG rhythms of two patients with hemiplegia.

Our preliminary study showed that the Tucker model can produce a more compact representation of data than PARAFAC [11]. Interpretation of the four-way PARAFAC would be difficult when applied to data collected across different sessions. This is because the PARAFAC model assumes the same number of components in each mode. To adequately model variability of the time activation of a given atom across different sessions, it would be required to set the number of components in the PARAFAC model to be several times higher than the number of sessions. This would lead to an unnecessarily complex model with difficult interpretability of the extracted components. On the other hand, a flexible Tucker model with appropriate restrictions is applicable also in the case of multi-session recordings. Therefore, in this study, we focus on the Tucker model only,

[1] This approach can be interpreted as an unfolding of a four-way tensor [2].

and we validate and compare our results with subject-specific atoms previously obtained by applying PARAFAC to each session separately.

2 Data

Multi-channel EEG data of two patients with right-hand hemiplegia recorded over twenty-four and eight motor imagery-based neurorehabilitation training sessions with the robotic splint were used in the study [8]. During the training blocks, a trained technician recorded EEG continuously using 12 active Ag/AgCl electrodes embedded in an elastic fabric cap (g.GAMMAcap; g.tec medical engineering, Schiedlberg, Austria). The technician placed the electrode cap on the participant's head according to the manufacturer's instructions, attaching six active EEG left-side scalp electrodes (FC3, C1, C3, C5, CP3, and O1), six active right-side electrodes (FC4, C2, C4, C6, CP4, and A2), one reference electrode (A1), and one ground electrode (AFz). Later, for signal processing, we used the signal from the A2 electrode to re-reference all EEG recordings to the average earlobe [(A1+ A2)/2] signal. A 16-channel g.USBamp system (g.tec medical engineering), with the sampling rate 128 Hz served to record all EEG signals.

We performed initial analyses using the BrainVision Analyzer 2 software (Brain Products, GmbH). This involved automatic artifact detection with criteria of maximally allowed voltage step 50 μV/ms, lowest allowed activity in intervals of 100 ms set to 0.5 μV, and maximally allowed difference of voltages in intervals of 20 ms set to 50 μV. If any of the first two criteria were met, the interval preceding and following the detected artifact by 150 ms was marked as bad. In the case of the third criterion, this interval was set to 50 ms. Next, using the same software, a trained technician visually inspected EEG data and detected artifacts. The technician manually marked periods with undetected artifacts and removed artifact markers wrongly assigned automatically. This included the detection and removal of ocular artifacts.

The EEG signal was then segmented into two-second time windows with 250 ms of overlap. For each time window, the oscillatory component of the amplitude spectrum was estimated by the irregular resampling auto-spectral analysis (IRASA) [13]. Possible negative spectral densities of the oscillatory part estimate were set to zero and a value of one was added before performing the logarithmic transformation with a base of ten. Obtained logarithmic spectral data in the frequency range of 4 to 25 Hz and with the 0.5 Hz frequency resolution were re-arranged into:

i) a four-way tensor $\mathbb{X}_{(4)} \in \mathbb{R}_{+}^{I_1 \times I_2 \times I_3 \times I_4}$ (*time* × *electrodes* × *frequencies* × *sessions*)
ii) three-way tensors $\mathbb{Y}_l \in \mathbb{R}_{+}^{I_1 \times I_2 \times I_3}, l = 1, \ldots, I_4$ (*time* × *electrodes* × *frequencies*), which were concatenated across the first mode into the final three-way tensor $\mathbb{X}_{(3)} \in \mathbb{R}_{+}^{I_1 I_4 \times I_2 \times I_3}$.

The tensors $\mathbb{X}_{(4)}$ and $\mathbb{X}_{(3)}$ were centred across the first mode. To detect a subject-specific oscillatory activity, the tensors were constructed and analysed for each subject separately.

3 Methods

The N-way Tucker model [12] decomposes an N-way tensor $\mathbb{X} \in \mathbb{R}^{I_1 \times I_2 \times \cdots \times I_N}$ into matrices $A^{(n)} \in \mathbb{R}^{I_n \times J_n}, n = 1, \ldots, N$ and a core tensor $\mathbb{G} \in \mathbb{R}^{J_1 \times J_2 \times \cdots \times J_N}$

$$X_{i_1,i_2,\ldots,i_N} = \sum_{k=1}^{N} \sum_{j_k=1}^{J_k} g_{j_1,j_2,\ldots,j_n} a^{(1)}_{i_1 j_1} a^{(2)}_{i_2 j_2} \ldots a^{(N)}_{i_N j_N} + e_{i_1,i_2,\ldots,i_N} \tag{1}$$

by minimising the sum of squared residuals.[2] The tensor

$$\mathbb{E} = (e_{i_1,i_2,\ldots,i_N})_{\substack{i_k=1,\ldots,I_k \\ k=1,\ldots,N}} \in \mathbb{R}^{I_1 \times I_2 \times \cdots \times I_N}$$

represents the noise term. The factor matrices $A^{(n)}, n = 1, \ldots, N$ are constrained to have normalised columns.

In the study, we consider a four-way Tucker model (next denoted as Tucker4D) for $\mathbb{X}_{(4)}$ and a three-way Tucker model (Tucker3D) for the tensor $\mathbb{X}_{(3)}$. In both cases, the factor matrices $A^{(1)}, A^{(2)}, A^{(3)}$ represent *time scores* (TS), *spatial signatures* (SS) and *frequency signatures* (FS), respectively. An atom's activation in time is represented by a single or a linear combination of TS with weights equal to the corresponding elements of G.

In Tucker4D, the matrix $A^{(4)}$ characterises the presence of atoms across sessions. However, as highlighted in the Introduction section, sessions do not share common patterns in the time domain. In other words, atoms sharing the same FS and SS should follow their own time scores for different sessions. Consequently, $A^{(4)}$ should be a fixed matrix with a diagonal structure. However, due to the unit norm assumption of the matrix columns, $A^{(4)}$ is considered as an $(I_4 \times I_4)$-dimensional identity matrix.

To improve the stability and interpretability of the Tucker decomposition, it is recommended to constrain the solution following the character of the analysed data [6]. Due to the fact that our data represent a positive log_{10}-transformed oscillatory part of the amplitude spectrum, we assumed the matrices $A^{(2)}, A^{(3)}$ to be non-negative. Because we focus on extracting sources of narrow-band oscillations, the columns of $A^{(3)}$ were constrained to be unimodal. Following our previous studies [9,11], the matrix $A^{(1)}$ in Tucker3D was set to be non-negative. For Tucker4D, we considered two alternatives for $A^{(1)}$ – non-negativity and orthogonality. In the following text, these two versions of Tucker4D are denoted as Tucker4D_N and Tucker4D_O.

In [11], we observed an improvement in the physiological interpretation and stability of the Tucker model decomposition with the non-negative constraint on elements of the core tensor $\mathbb{G}$. This was true in comparison to the model with an unconstrained $\mathbb{G}$ structure. Following this result, we set the core tensor $\mathbb{G}$ to be non-negative in all Tucker3D and Tucker4D model variants also in this study.

[2] The PARAFAC model also follows the formula (1), but with the assumption of the same number of factors in each mode ($J_1 = \cdots = J_N = J$) and a super–diagonal structure of $\mathbb{G}$.

Two stable SS patterns representing EEG oscillatory sources in the left or right hemisphere were observed in [11]. Therefore, in the current study, the number of SS was also set to two ($J_2 = 2$). We varied the number of frequency signatures (J_3) between 8 and 11. Also, following our previous experience and results [11], the number of TS was varied between J_3 and $2 * J_3$. This follows the observation that the majority of atoms in the left and right hemisphere often show different time activation.

The variation of these parameters leads to a set of solutions (runs). Instead of choosing one final Tucker model for a subject, we investigated all solutions whose core consistency diagnostics (CCD) [1] was greater than 0.5. When validating solutions of the Tucker3D and Tucker4D models we focused on the

- comparison of time, spatial and frequency characteristics of atoms obtained from the models
- maximum number of factors necessary to adequately describe data structure variability
- presence of stable atoms across solutions and their comparison with the subject-specific atoms already known from applying the PARAFAC model to each training session separately.

4 Results

An example of the Tucker3D model with 16 TS and 8 FS is depicted in Fig. 1. The model detected eight oscillatory rhythms with the peak frequencies at 6.5, 8, 9.5, 11, 13, 14.5, 16.5, and 19.5 Hz (Fig. 1, first row). Spatial signatures represent the location of these oscillatory EEG sources either in the left or right hemisphere (Fig. 1, first and second row, two right plots). The core tensor $\mathbb{G}$ slices represent the relationship between SS and TS for a given atom (Fig. 1, second row, left). For example, the time activation of the left 8 Hz EEG rhythm across all sessions corresponds to the 6^{th} TS. For the right hemisphere, it is the 10^{th} TS.

The interpretation and visualisation of the Tucker4D model is similar, however, in this case, $\mathbb{G}$ represents a four-way core tensor.

For both subjects, the core tensor $\mathbb{G}$ of the Tucker3D and Tucker4D_N models showed a sparse structure. For Subject 1 this is depicted in Fig. 1 (second row) and Fig. 2 (top and middle rows). Consequently, the time activation of the extracted atoms is equal to one TS (a column of $A^{(1)}$) or to a linear combination of a few of them. However, their interpretation differs between three- and four-way models. For Tucker3D, the time scores are vectors with the length $I_1 * I_4$ and they represent the time activation across all sessions, but for Tucker4D_N they characterise only one session.

Due to the sparse structure of $\mathbb{G}$, the optimal number of time scores for the Tucker3D model is approximately $J_2 * J_3 = 2 * J_3$. But for Tucker4D_N it is $J_2 * J_3 * k, k \approx J_4$. However, in this study, we considered J_1 to be at most $2 * J_3$, and therefore the Tucker4D_N model did not have enough TS to adequately describe data structure variability. Consequently, the model shows a significantly higher mean squared error (MSE) in comparison to Tucker3D,

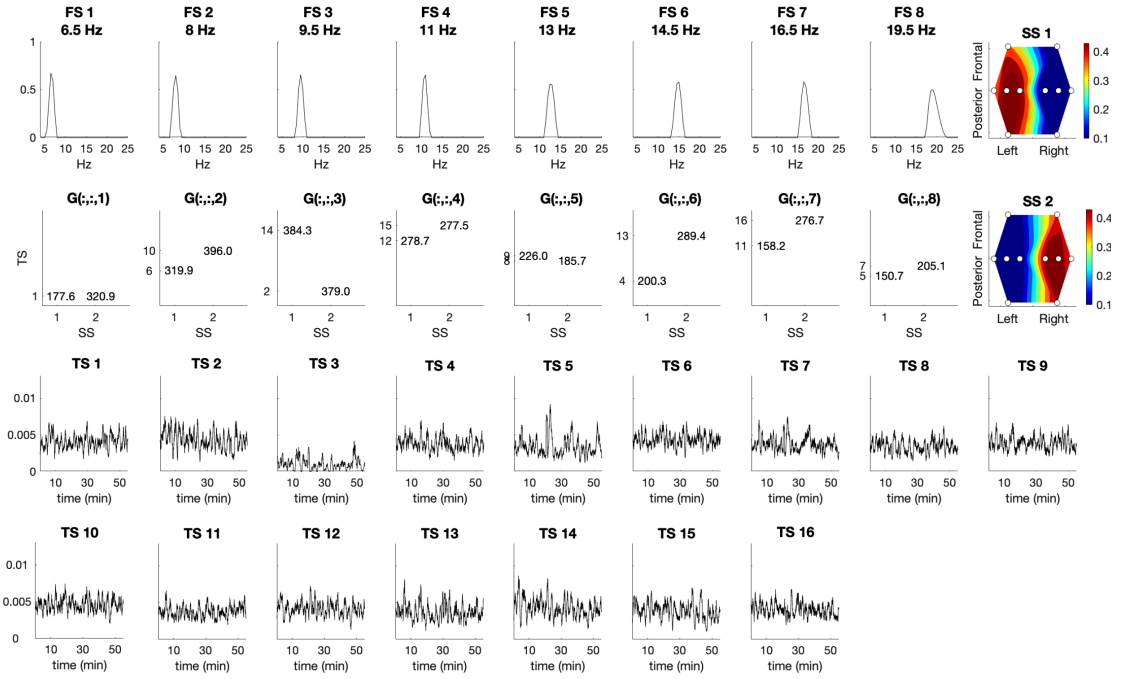

Fig. 1. Subject 1. An example of the Tucker3D model with eight frequency signatures (FS, first row), two spatial signatures (SS, first and second row, two right plots) and 16 time scores (TS, third and fourth row). Non-zero elements in slices of the core tensor $\mathbb{G}$ for a given FS are depicted in the second row on the left (Color figure online).

but also when compared with the Tucker4D_O model (Fig. 3). Naturally, an improvement can be achieved by increasing the number of TS, but this would be at the cost of longer computation time, numerical and convergence problems as well as leading to higher complexity of the model.[3] Therefore, we conclude that the Tucker4D_N model may not be appropriate when used in the studied multi-session EEG recording scenario and was not further analysed.

In contrast to Tucker3D and Tucker4D_N, the core tensor $\mathbb{G}$ after the convergence turned to be dense in the case of the Tucker4D_O models (Fig. 2, bottom). In the Tucker4D_O model, the columns of $A^{(1)}$ form an orthogonal basis and can not be interpreted directly. More attention needs to be paid to each particular linear combination of the $A^{(1)}$ columns representing the final time activation of an atom in a given session.

A comparison of time activation of 8 Hz right hemisphere oscillatory atom for a randomly chosen session and solution of the Tucker4D_O and Tucker3D models is depicted in Fig. 4a. The observed differences between curves are due to different constraints applied to $A^{(1)}$ in each of the two models. However, and most importantly, the dynamic of both curves is very similar. Because the overall dynamic profiles of time scores, and not their absolute values are in our focus,

[3] For Subject 1, fixing the number of FS to eight and SS to two, the Tucker4D_N model with eighty TS shows MSE approximately of the same value as the Tucker4D_O model with sixteen TS.

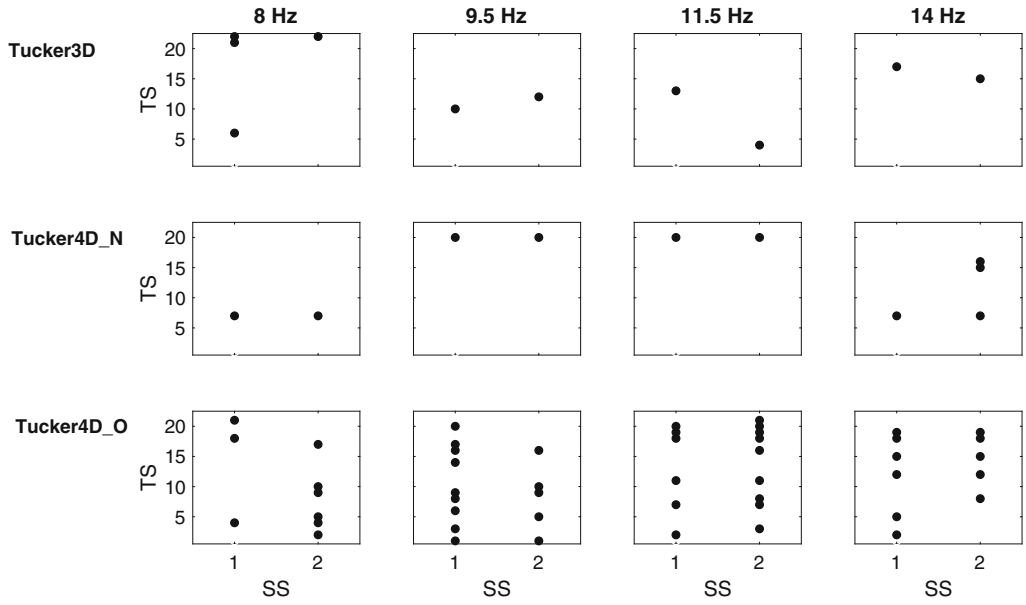

Fig. 2. Subject 1. Slices of the core tensor $\mathbb{G}$ for oscillatory atoms with the peak frequencies at 8, 9.5, 11.5, and 14 Hz of the Tucker3D (top row), Tucker4D_N (second row) and Tucker4D_O (third row) models. Slices over the first session are depicted in the case of the Tucker4D_N and Tucker4D_O models. The Tucker3D and both variants of the Tucker4D model were run with 22 time scores (TS), 2 space signatures (SS) and 11 frequency signatures (FS). Only the non-zero elements of the core tensor $\mathbb{G}$ slices are depicted (black circles).

we can conclude that both versions of the Tucker model led to comparable time activation profiles.

Spatial signatures from all solutions (runs with different parameter settings) of the Tucker3D and Tucker4D_O models are depicted in Fig. 4b. Similarly to [11], SS represent the spatial distribution of the oscillatory EEG activity either in the left or right hemisphere. We observed high stability of these SS across all runs and models.

Finally, we investigated the detectability and stability of FS across different runs. For this purpose, DBSCAN [4], a density-based clustering method, was applied to FS solutions of both Tucker3D and Tucker4D_O models.

For Subject 1, the dominant clusters of FS of the Tucker3D and Tucker4D_O models represent EEG oscillatory activity with the peak frequencies at 8, 9.5, 11.5, 14, and 15.5 Hz (Fig. 5a, middle, and bottom) and are consistent with FS of the subject-specific atoms already detected by PARAFAC applied to each training session separately (Fig. 5a, top).

The difference between considered approaches occurred only for rhythms with higher frequencies (in the range of 17 to 19 Hz). The Tucker4D_O model FS form a cluster with the peak frequency at 17.5 Hz, which is consistent with the PARAFAC results, but the corresponding Tucker3D model cluster indicates a slight shift of the peak frequency of this atom to 16.5 Hz. The rhythm with the peak frequency close to 19 Hz was detected in several runs of the two

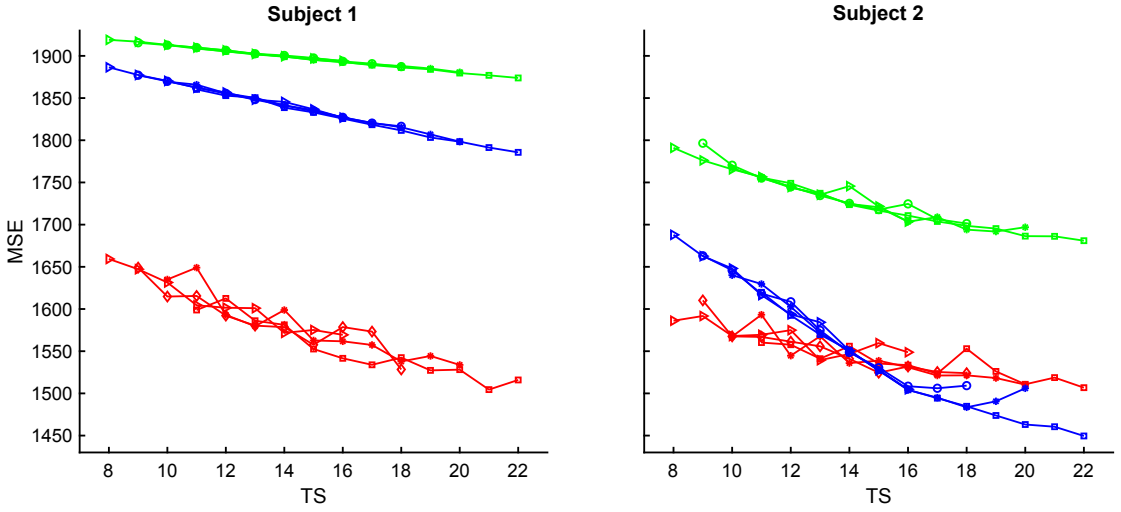

Fig. 3. Mean squared error (MSE) for the Tucker3D (red), Tucker4D_N (green) and Tucker4D_O (blue) model runs for which the core consistency diagnostics was greater than 0.5. In all models, the number of spatial signatures was set to two, the number J_3 of frequency signatures was set to 8 ($\triangleright$), 9 ($\diamond$), 10 ($*$) or 11 ($\square$) and the number of time scores (TS) varied between J_3 and $2 * J_3$ (Color figure online).

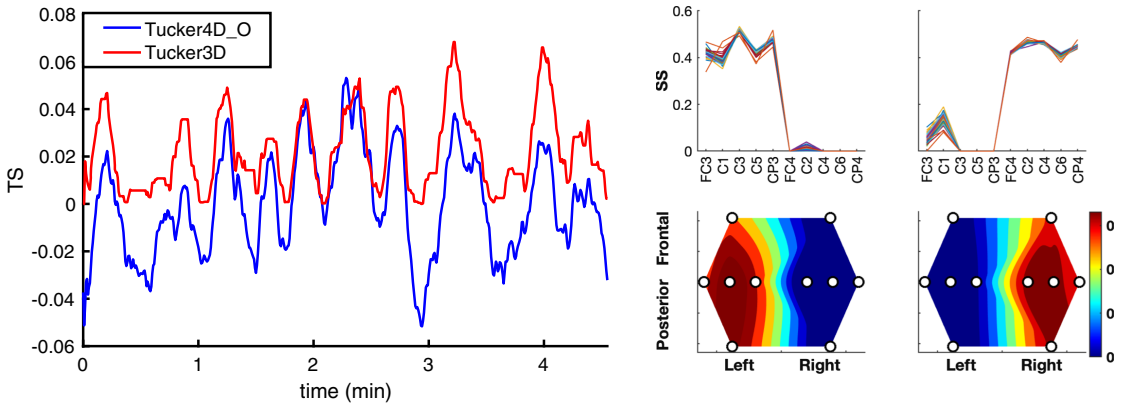

(a) (b)

Fig. 4. Subject 1. (a) Time scores (TS) for 8 Hz oscillatory EEG activity in the right hemisphere for a randomly chosen solution of the Tucker4D_O (blue) and Tucker3D (red) models. (b) *Top*: Spatial signatures (SS) from all runs of the Tucker4D_O and Tucker3D models representing spatial distribution of the oscillatory EEG activity in the left and right hemisphere over the sensorimotor cortex. *Bottom*: scalp topographic map of the average of SS depicted in the top plot. (Color figure online)

models (Fig. 1), but a stable cluster was identified neither in Tucker3D nor in Tucker4D_O.

Subject 2 specific atoms detected by PARAFAC show the peak frequencies at 8, 9.5, 11, 13.5, 16, and 17 Hz. The dominant clusters of FS for both Tucker4D_O and Tucker3D indicate the peak frequencies at 7.5, 9-9.5, 11, and 13-13.5 Hz (Fig. 5b).

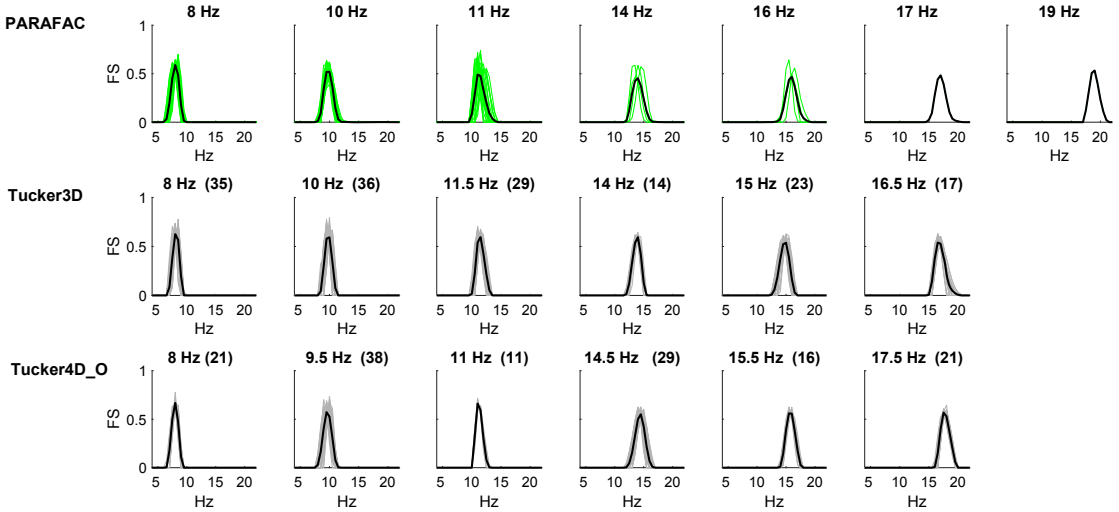

(a) Subject 1

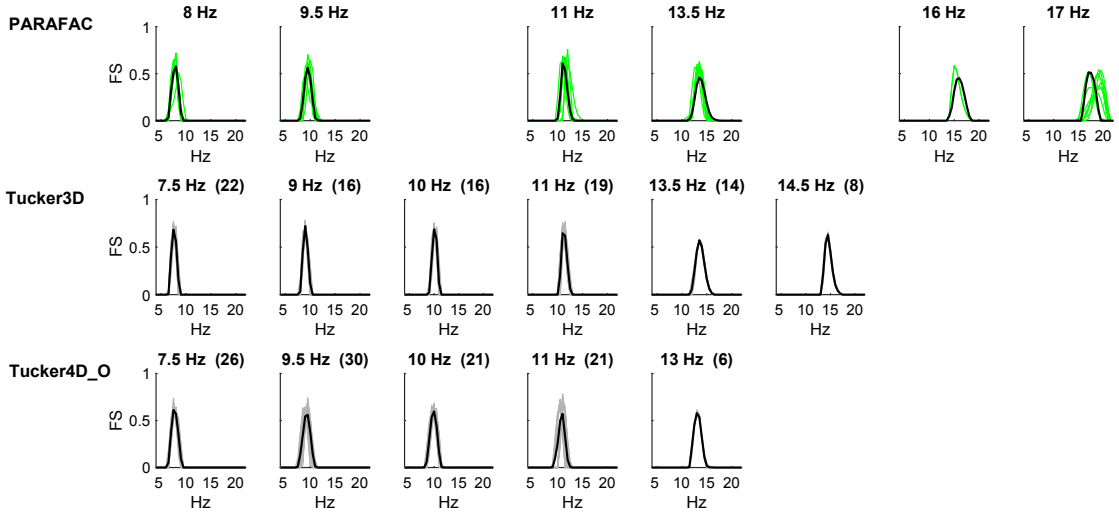

(b) Subject 2

Fig. 5. Frequency signatures (FS) of the atoms detected by the DBSCAN cluster analysis. For each subject, the PARAFAC (top row), Tucker3D (middle row), and Tucker4D_O (bottom row) solutions are depicted. The grey curves represent cluster elements for the Tucker models (individual solutions), the cluster representative (black bold curve) was computed as an average of all solutions. In the title of each subplot, the number of elements in each cluster is depicted in parenthesis. For PARAFAC, the cluster analysis was applied within each session separately. Cluster representatives for each session are depicted in green, the black bold curve represents their average (Color figure online).

The rhythms at 16 and 17 Hz formed stable clusters neither in Tucker3D nor in Tucker4D_O. However, when looking at the results of PARAFAC and cluster analysis applied to each session separately (Fig. 5b), the atom with the peak frequency 16 Hz was present only in five of the eight sessions. The 17 Hz atom was also not stable, and for several sessions its peak frequency was shifted

slightly upward (Fig. 5b, last figure in the top row). We hypothesise that the failure of the Tucker model to detect the two atoms is caused by their smaller activation in some sessions and by the fact that the Tucker model focuses on atoms that show a higher variability across all sessions.

On the other hand, a stable cluster representing EEG oscillatory activity peaked at 10 Hz occurred in both Tucker models, but not in the case of the PARAFAC model. Both identified rhythms at 9-9.5 Hz and 10 Hz are very close in frequency and the results of both Tucker models indicate a possible frequency variation of this rhythm across individual sessions. Previous analysis using EEG data recorded at the occipital O1 site during the resting state eyes closed and eyes open conditions indicates that the atom represents the posterior visual alpha rhythm. However, further session to session, as well as a higher frequency and spatial resolution analysis would be needed to confirm the relevance of this physiological interpretation of the rhythm.

5 Conclusion

The benefit of the tensor decomposition methods for the extraction of narrow-band oscillatory rhythms from EEG records of patients after ischemic stroke has been already demonstrated [9,10]. However, the neurorehabilitation sessions were analysed separately and the subject-specific atoms were detected in a separate semi-automatic step consisting of cluster analysis and visual inspection of the results [10]. As both procedures are time-consuming, especially for subjects with a higher number of sessions, we search for a more efficient approach.

In the study, we dealt with a simultaneous analysis of the multi-channel EEG recorded during multiple sessions (days) of the motor imagery-based neurofeedback training of two patients with hemiplegia. Two approaches were considered

- Tucker4D: the four-way Tucker model, either with non-negative or orthogonal time factor matrix $A^{(1)}$, and applied to data arranged into of a four-way tensor
- Tucker3D: the three-way model with unfolded data from all sessions across the time mode resulting in one large three-way tensor.

The benefit of the Tucker3D model in comparison to PARAFAC was already demonstrated in [11]. However, we observed a practical disadvantage of the model. The Tucker model algorithm is based on the Kronecker products [2]. For tensors with one mode of a large size, the Kronecker product matrices are large in size and they can require up to several GB of computer memory. Therefore, an appropriate optimisation of the algorithm may be needed if the number of analysed sessions grows. To address this problem, in this study, we also investigated the Tucker4D model, where the memory allocation is reduced.

For Tucker4D_N, the assumption of the non-negative time scores matrix $A^{(1)}$ showed to be inappropriate. The model showed significantly higher MSE than the Tucker3D and Tucker4D_O models. An improvement can be achieved by increasing the number of components to a multiple of the number of sessions. However, that leads to an unnecessarily complex model and possible numerical

problems. Better results were observed for the alternative four-way Tucker4D_O model in which the columns of $A^{(1)}$ formed an orthogonal basis. In this case, the number of time scores was chosen to be at most $2 * J_3$. Using the estimated elements of the core tensor $\mathbb{G}$, the weighted linear combinations of the $A^{(1)}$ columns then represent the final time activation for an arbitrary atom.

The Tucker3D and Tucker4D_O models produced consistent results when validating obtained spatial and frequency signatures, as well as time scores. But what is more important, in both cases we were able to detect stable atoms which were consistent with the subject-specific atoms already detected by a combination of the PARAFAC model and a cluster analysis applied to each training session separately [10,11]. This was especially true for slower frequency rhythms (7 to 15 Hz), which are in the focus of the studied motor imagery related changes of EEG oscillatory activity.

We can conclude that both approaches showed comparable and adequate results when applied to the simultaneous analysis of multi-session recordings of multi-channel EEG. When the subject-specific atom extraction is in the focus, they provide a time-saving alternative to the tensor decomposition applied to each session separately.

Acknowledgment. This research was supported by the Slovak Research and Development Agency (grant APVV-16-0202) and by the VEGA grant 2/0081/19.

References

1. Bro, R., Kiers, H.A.L.: A new efficient method for determining the number of components in PARAFAC models. J. Chemom. **17**(5), 274–286 (2003). https://doi.org/10.1002/cem.801
2. Cichocki, A., Zdunek, R., Phan, A.H., Amari, S.I.: Nonnegative Matrix and Tensor Factorizations: Applications to Exploratory Multi-way Data Analysis and Blind Source Separation. Wiley, New York (2009). https://doi.org/10.1002/9780470747278
3. Cong, F., Lin, Q.H., Kuang, L.D., Gong, X.F., Astikainen, P., Ristaniemi, T.: Tensor decomposition of EEG signals: a brief review. J. Neurosci. Methods **248**, 56–69 (2015). https://doi.org/10.1016/j.jneumeth.2015.03.018
4. Ester, M., Kriegel, H.P., Sander, J., Xu, X.: A density-based algorithm for discovering clusters in large spatial databases with noise. In: Proceedings of the Second International Conference on Knowledge Discovery and Data Mining (KDD-96), pp. 226–231. AAAI Press (1996)
5. Harshman, R.A.: Foundations of the PARAFAC procedure: models and conditions for an "explanatory" multimodal factor analysis. In: UCLA Working Papers in Phonetics, vol. 16, no. 1 (1970)
6. Kiers, H.A.L.: Recent developments in three-mode factor analysis: constrained three-mode factor analysis and core rotations. In: Hayashi, C., Yajima, K., Bock, H.H., Ohsumi, N., Tanaka, Y., Baba, Y. (eds.) Data Science, Classification, and Related Methods. STUDIES CLASS, pp. 563–574. Springer, Tokyo (1998). https://doi.org/10.1007/978-4-431-65950-1_62

7. Miwakeichi, F., Martınez-Montes, E., Valdés-Sosa, P.A., Nishiyama, N., Mizuhara, H., Yamaguchi, Y.: Decomposing EEG data into space-time-frequency components using Parallel Factor Analysis. NeuroImage **22**(3), 1035–1045 (2004). https://doi.org/10.1016/j.neuroimage.2004.03.039
8. Rosipal, R., Porubcová, N., Cimrová, B., Farkaš, I.: Neurorehabilitation training based on mental imagery of movement (using a robotic splint) (2017). http://aiolos.um.savba.sk/~roman/rrLab/projects.html
9. Rosipal, R., Porubcová, N., Barančok, P., Cimrová, B., Farkaš, I., Trejo, L.J.: Effects of mirror-box therapy on modulation of sensorimotor EEG oscillatory rhythms: a single-case longitudinal study. J. Neurophysiol. **121**(2), 620–633 (2019). https://doi.org/10.1152/jn.00599.2018
10. Rošťáková, Z., Rosipal, R.: Three-way analysis of multichannel EEG data using the PARAFAC and Tucker models. In: 12th International Conference on Measurement, Smolenice, Slovakia, pp. 127–130 (2019). https://doi.org/10.23919/MEASUREMENT47340.2019.8780005
11. Rošťáková, Z., Rosipal, R., Seifpour, S., Trejo, L.J.: A comparison of non-negative Tucker decomposition and parallel factor analysis for identification and measurement of human EEG rhythms. Meas. Sci. Rev. **20**(3), 126–138 (2020). https://doi.org/10.2478/msr-2020-0015
12. Tucker, L.R.: Some mathematical notes on three-mode factor analysis. Psychometrika **31**(3), 279–311 (1966). https://doi.org/10.1007/BF02289464
13. Wen, H., Liu, Z.: Separating fractal and oscillatory components in the power spectrum of neurophysiological signal. Brain Topogr. **29**(1), 13–26 (2015). https://doi.org/10.1007/s10548-015-0448-0